ARTICLE

Prediction of water quality effect on saturated hydraulic conductivity of soil by artificial neural networks

M. Khataar[1] · **M. R. Mosaddeghi[2]** · **Reza Amiri Chayjan[3]** · **A. A. Mahboubi[4]**

Abstract

This study was conducted to investigate the impact of water salinity (EC_w) and sodicity (SAR_w) on saturated (K_s) and relative (K_r) hydraulic conductivities in two clay (C) and sandy clay loam (SCL) soils. The results showed that the K_s decreased with increasing SAR_w, and in all of water quality treatments, the K_s of SCL soil was higher than that of the C soil. Sodicity effect (even at high SAR_w) on the K_r of clay soil was minimized by high salinity. Although K_r of both soils similarly responded to EC_w and SAR_w, microstructure of clay soil was more sensitive to water quality. Effect of EC_w on soil structure was greater than that of SAR_w. In order to assess the applicability of artificial neural networks (ANNs) in estimating K_s and K_r, two types of FFBP and CFBP ANNs and two training algorithms, namely Levenberg–Marquardt (LM) and Bayesian regulation, were employed with two strategies of uniform threshold and different threshold functions. Multiple linear regressions were also used for K_s and K_r prediction. Based on the ANN results of second strategy, best topology (4–5–4–1) was belonged to CFBP network with LM algorithm, LOGSIG–LOGSIG–TANSIG threshold functions, and values of MAE and R^2 are equal to 0.1761 and 0.9945, respectively. Overall, the efficacy of ANNs is much greater than regression method for K_s prediction.

Keywords Artificial neural networks · Salinity · Soil hydraulic conductivity · Water quality

Introduction

Hydraulic conductivity (K) is one of the important physical properties of soil which depends on soil pores continuity, tortuosity and distribution (Mossadeghi-Björklund et al. 2016). Irrigation with low-quality waters is common in arid and semiarid regions and may reduce the soil hydraulic conductivity. Swelling, aggregate failure, pore-size reduction, partial blocking and dispersion of clays are induced by the irrigation with low-quality waters and ultimately affect the soil hydraulic conductivity (Bagarello et al. 2006; Bourazanis et al. 2016). It was reported that K is very sensitive indicator to detect changes in soil porosity caused by sodicity increment (Keren and Ben-Hur 2003). An increase in soil sodium adsorption ratio (SAR), by effluent irrigation, resulted in enhanced clay swelling and dispersion and decreased the saturated hydraulic conductivity (K_s) (Lado and Ben-Hur 2009; Bourazanis et al. 2016), aggregate stability, and surface crusting and low-quality tilth (Suarez et al. 2006). In the absence of electrolytes, the impact of fast wetting (slaking) and swelling on the hydraulic conductivity was most notable, mainly at the intermediate sodicity levels (ESP = 5–10) (Levy et al. 2005). The use of saline water significantly reduced the impact of fast wetting and swelling on the hydraulic conductivity. Results suggested that combined effects of salinity, wetting rate and sodicity on the hydraulic conductivity were complex and should thus be considered simultaneously when estimating soil hydraulic conductivity (Levy et al. 2005).

✉ M. Khataar
mahnazkhataar@znu.ac.ir

M. R. Mosaddeghi
mosaddeghi@cc.iut.ac.ir

Reza Amiri Chayjan
amirireza@basu.ac.ir

A. A. Mahboubi
mahboubi@uoguelph.ca

[1] Department of Soil Science, University of Zanjan, Zanjan 38791-45371, Iran

[2] Department of Soil Science, College of Agriculture, Isfahan University of Technology, Isfahan 84156-83111, Iran

[3] Department of Biosystems Engineering, College of Agriculture, Bu-Ali Sina University, Hamadan 65174, Iran

[4] School of Engineering, University of Guelph, Guelph, ON, Canada

Artificial neural networks

Artificial neural networks (ANNs) have been extensively employed as an artificial intelligence method for modeling and prediction purposes. The ANN uses simple processing elements named neurons which have been related to special arrangement. An ANN tries to discover the inherent relationships between input and output parameters through learning process. Hidden layer(s) process the input data from input layer and produce answer in output layer. Each network is trained with real patterns. During this process, the connection weights between layers are changed until the errors between predicted values and the target (experimental values) are reduced to a permissible value (Heristev 1998).

Multilayer perceptron (MLP) networks are the most robust and popular types of ANNs for prediction of variables in engineering sciences (Raheli et al. 2017). Two well-known types of MLP networks are FFBP and CFBP (Kaveh et al. 2017). LM and BR are the best training algorithms with the lowest training epoch (Love 2017). These algorithms are the newest methods for training of the MLP networks (Chayjan and Esna-Ashari 2010). Advantages and features of FFBP and CFBP networks and LM and BR algorithms are described in the sections of "Network types" and "Training algorithms."

Network types

(a) Feed-forward back propagation (FFBP): This network consists of one input layer, one or several hidden layers and one output layer. Usually, back-propagation (BP) learning algorithm is used to train this network (which finally results in learning). During the training of this network, calculations were carried out from input of network toward the output, and then, the values of error were propagated to prior layers. Output calculations were carried out by layer to layer, and the output of each layer is the input of next layer (Demuth et al. 2007).

(b) Cascade-forward back propagation (CFBP): This network like FFBP network uses the BP algorithm for updating weights, but the main characteristic of this network is that each layer's neuron is related to all the previous layer neurons.

Training algorithms

Two training algorithms are used for updating the network weights. These algorithms are Levenberg–Marquardt (LM) and Bayesian regulation (BR) algorithms:

(a) LM algorithm: The LM algorithm is a Hessian-based algorithm for nonlinear least squares optimization. Hessian-based algorithms allow the network to learn features of a complicated mapping more suitably. The training process converges quickly as the solution is approached, because the Hessian does not vanish at the solution.

(b) Bayesian regularization (BR) algorithm: In this algorithm, instead of the sum of squared error (SSE) on the training set, a cost function, which is the SSE plus a penalty term, is automatically adjusted (Girosi et al. 1995).

The ANNs have been extensively employed in soil science as pedotransfer functions (PTFs) for prediction of hardly available properties using easily available properties. With adequate and sensitive data, ANN can be used to estimate, for example, K_s, using easily available soil properties such as sand, silt, and clay content, bulk density, and organic carbon content (Agyare et al. 2006). Parasuraman et al. (2006) compared the performance of the field-scale PTF_s with an available ANN program and Rosetta methods, namely bagging and boosting in estimating K_s. They showed that the field-scale models performed better than Rosetta. The ANN model employing the boosting algorithm results in better generalization by reducing both the bias and variance of the ANN models. Lim and Kolay (2009) compared Shepard's equation and ANN method for estimation of K. The results showed that the trained network consistently produced most accurate predictions ($R^2 = 0.8493$). The study of Erzin et al. (2009) deals with development of ANNs and multiple regression analysis (MRA) models for predicting hydraulic conductivity of fine-grained soils. The ANN models better predicted the K than the MRA models based on selected performance indices. It was demonstrated that the developed ANN models could be employed for predicting hydraulic conductivity of compacted fine-grained soils quite efficiently.

Quality of irrigation waters is usually low (i.e., high EC and/or SAR) in most arid and semiarid regions (Emdad et al. 2004). There are few documentations about the influences of water quality on soil hydraulic properties, but the information on the impacts of water quality on calcareous soils which are widespread in Iran is scanty. Moreover, water quality effects on soil hydraulic properties were rarely predicted using ANNs so far. The objectives of this study were: (1) to assess the effect of water quality on saturated hydraulic conductivity (K_s) of two clay and sandy clay loam soils from western Iran, and (2) to predict the effect of soil type and water quality on K_s using regression and ANNs methods.

Materials and methods

Soils and water quality treatments

Two non-saline and non-sodic agricultural soils were selected in Hamadan province, western Iran. The soil samples were carefully collected at a suitable water content from 0 to 30 cm layer to avoid the destruction of soil aggregates. Some of the samples were air-dried, ground and passed through a 2-mm mesh sieve. Particle size distribution was determined using the hydrometer. Particle density was measured by the pycnometer method (Klute 1986). Soil electrical conductivity (EC) and pH were determined with an EC meter (Metrohm 712) and a pH meter (Metrohm 744) using 1:5 soil/water suspension, respectively. Carbonate content was measured using the back-titration method. Organic matter content was determined using the wet-digestion method (Page et al. 1992). Some physical and chemical properties of the soils are given in Table 1.

Water quality treatments comprised all combinations of water EC (EC_w) values of 0.5, 2, 4 and 8 dS m^{-1} and SAR_w values of 1, 5, 13 and 18 (meq l^{-1})$^{0.5}$ (in total 16 solutions). Pure NaCl and CaCl$_2$ salts (Merk) were used to prepare the solutions. Distilled water was used as control. The following two equations are used to prepare the solutions with desired EC_w and SAR_w:

$$TA_w = TC_w = 10 \times EC_w \tag{1}$$

$$SAR_w = \frac{[Na^+]}{\sqrt{\frac{Ca^{2+}}{2}}} \tag{2}$$

where TA_w and TC_w refer to total anion and total cation concentrations both in meq l^{-1} and [Na$^+$] and [Ca^{2+}] stand for concentrations (meq l^{-1}) of sodium and calcium ions in the solutions. Equations (1) and (2) are solved with the mentioned EC_w and SAR_w values to calculate [Na$^+$] and [Ca^{2+}] and the amounts of NaCl and CaCl$_2$ salts and to prepare the 16 solutions. The EC_w of the prepared solutions was tested for correctness of calculations and checking purity of the salts.

Soil preparation

Some of the collected soils were air-dried and sieved through 2-mm mesh without grinding and/or breaking the soil aggregates in order to preserve the micro-aggregates in the soil mass. The soils were packed into cylinders (with 7 cm height and 5 cm diameter) to 6 cm thickness and to have an initial similar void ratio of 1.2 (i.e., porosity of 0.55). The initial pore volume (PV) of all the soil samples was 76.6 cm^3. In total, 16 solutions × 2 soil types in three replicates (in total 96 soil cores) were prepared.

Leaching setup and saturated hydraulic conductivity measurement

All of the soil columns were initially saturated by distilled water. The K_s of the soil columns was measured using the constant-head method (Levy et al. 1999). The constant head on the columns was maintained using the Marriott burette technique. The solution reservoir was filled with a solution having specific EC_w and SAR_w, and the leaching was started to monitor the effect of water quality on the K_s during the leaching time.

The K_s (cm h^{-1}) is calculated using the Darcy's equation as follows:

$$K_s = \frac{V_w}{A \Delta t} \times \frac{L}{\Delta \psi_h} \tag{3}$$

where V_w is the cumulative volume (cm^3) of effluent in the time interval (Δt, h), A is the cross-sectional area (cm^2) of soil column, $\Delta \psi_h$ is the difference in hydraulic potential (cm) between top and bottom of the soil column and L is the length (cm) of soil column.

The leaching was continued for four times of soil column PV (4PV) or cumulative effluent volume of 306.4 cm^3. The K_s variation was measured with 0.25PV intervals.

In order to compare the effect of different treatments (soil type and water quality) on the hydraulic conductivity, relative hydraulic conductivity (K_r), as calculated using Eq. (4), is used:

$$K_r = \frac{K_s}{K_{s0}} \tag{4}$$

where K_{s0} is the saturated hydraulic conductivity at the beginning of leaching (i.e., at effluent volume of 0.25PV) as

Table 1 Physical properties of the studied soils

Soil series (location)	Clay (%)	Sand (%)	Texture	pH	OM (%)	EC (dS m^{-1})	CaCO$_3$ (%w/w)	PD (Mg m^{-3})
Hesam Abad	27.1	53.1	Sandy clay loam	7.59	1.87	0.198	15.0	2.57
Amir Abad	41.1	38.6	Clay	7.75	1.70	0.200	15.0	2.55

OM organic matter, *EC* electrical conductivity, *CaCO₃* calcium carbonate content, *PD* particle density

used by Green et al. (2003). The K_r values were also drawn versus PV.

Artificial neural networks

Structures and designing

Considering four inputs in all experiments (EC$_w$, SAR$_w$, soil texture or TEX and PV), the K_s and K_r values were derived for different conditions. Networks for K_s prediction with four neurons in the input layer (i.e., EC$_w$, SAR$_w$, TEX and PV) and one neuron in the output layer (K_s) were designed. Neural network toolbox of MATLAB software was used in this study (Sivanandam et al. 2006).

In order to obtain the desired answer, two networks of FFBP and CFBP for K_s prediction were utilized. Training process for these K_s networks was iterative. When the error between desired and predicted values became minimum, training process meets the stability. The increasing method was used for selecting layers and neurons for evaluation of various topologies. The increasing method has some advantages which are: (a) the network complexity gradually increases with increasing neurons; (b) the optimum size of the network always obtains by adjustments; and (c) monitoring and evaluation of local minimum carry out during the training process. Various threshold functions were used to reach the optimized status (Demuth et al. 2007):

$$Y_j = \frac{1}{1 + \exp(-X_j)} \quad \text{(LOGSIG)} \tag{5}$$

$$Y_j = \frac{1}{\left(1 + \exp(-2X_j)\right) - 1} \quad \text{(TANSIG)} \tag{6}$$

$$Y_j = X_j \quad \text{(PURELIN)} \tag{7}$$

where X_j is the sum of weighed inputs for each neuron in jth layer and computed as below:

$$X_j = \sum_{i=1}^{m} W_{ij} \times Y_j + b_j \tag{8}$$

where m is the number of output layer neurons, W_{ij} the weight between ith and jth layers, Y_i the ith neuron output and b_j bias of jth neuron for FFBP and CFBP networks. Experimental data of K_s and K_r were selected for training network with suitable topology and training algorithm and for testing of trained network.

The following criterion of root-mean-square error has defined to minimize the training error (Demuth et al. 2007):

$$\text{MSE} = \frac{1}{MN} \sum_{p=1}^{M} \sum_{i=1}^{N} \left(S_i - T_{ip}\right)^2 \tag{9}$$

where MSE is the mean square error, S_{ip} the network output in ith neuron and pth pattern, T_{ip} the target output at ith neuron and pth pattern, N the number of output neurons and M the number of training patterns. To optimize the selected network from prior stage, the secondary criteria were used as follows:

$$R^2 = -\frac{\sum_{k=1}^{n} \left[S_k - T_k\right]}{\sum_{k=1}^{n} \left[S_k - \frac{\sum_{k=1}^{n} S_k}{n}\right]} \tag{10}$$

$$E_{mr} = \frac{100}{n} \sum_{k=1}^{n} \left| \frac{S_k - T_k}{T_k} \right| \tag{11}$$

$$\text{SE} = \sum_{k=1}^{n} \sqrt{\frac{(S_k - T_k)^2}{\text{d.f.}}} \tag{12}$$

where R^2 is the coefficient of determination, E_{mr} the mean relative error, SE the standard error, S_k the network output for kth pattern, T_k the target output for kth pattern, d.f., degree of freedom and n the number of training patterns.

About 70% of all data were randomly selected for training of network with suitable topology and training algorithms. The remained data were used for validation and test.

Analysis of the data

The effect of soil type (texture) and water quality on the K_s and K_r at different PVs was assessed using statistical analysis in SAS software. The soil texture, EC$_w$ and SAR$_w$ were considered as treatments in a factorial arrangement of completely randomized design. Means of the K_r values were compared using Duncan's multiple range test. The K_s and K_r were predicted from the inputs of soil type, EC$_w$ and SAR$_w$ using multiple regression and artificial neural network (ANN) models. The statistical analysis was done using SAS software. Feed-forward and cascade forward networks and Levenberg–Marquardt and Bayesian regulation learning algorithms were utilized.

Results and discussion

### Effect of soil texture and water quality on K_s and K_r

The K_s is mainly dependent on soil macropores and pore continuity and decreases with destruction of macropores. The K_s values were greater in sandy clay loam soil (with larger pores) compared to clay soil. With an increase in SAR$_w$, the K_s decreased due to soil dispersion, macropore clogging by dispersed clay particles and clay swelling. These

effects depend on clay content and types; the finer the soil texture and the greater the amount of 2:1 clays, the greater will be clay dispersion and swelling. When soil is susceptible to dispersion and swelling, the soil structure will be damaged by sodicity (Levy et al. 2005). Buelow et al. (2015) observed that the importance of aggregate slaking in terms of soil hydraulic conductivity depended on both soil sodicity and clay content.

Figures 1 and 2 show the variation of K_r (averaged over replicates) versus PV for different water qualities and soil type treatments. The effect of SAR_w at low EC_w (i.e., 0.5 dS m^{-1}) on K_r variation of the clay soil is shown in Fig. 1a. It was observed that as leaching was continued (at high PV), the K_r decreased because the low-saline waters

could disperse the soil aggregates. This effect was greater when SAR_w increased. When the SAR_w reached to critical limit (i.e., about 13), the K_r decreased substantially, especially at initial PVs (Fig. 1a). There is an unexpected increase in K_r for SAR = 18, especially at high PVs presumably because of particles separation and creation of new pores upon extensive swelling.

The effect of SAR_w at moderate EC_w (i.e., 2 dS m^{-1}) on K_r variation of the clay soil is shown in Fig. 1b. When compared with Fig. 1a, it is concluded that the negative effect of SAR_w on K_r diminished when water salinity increases. The leaching effect with the moderately saline waters on K_r was even positive, especially at low SAR_w values (Fig. 1b). With salinity increase, the DDL thickness decreases and the soil
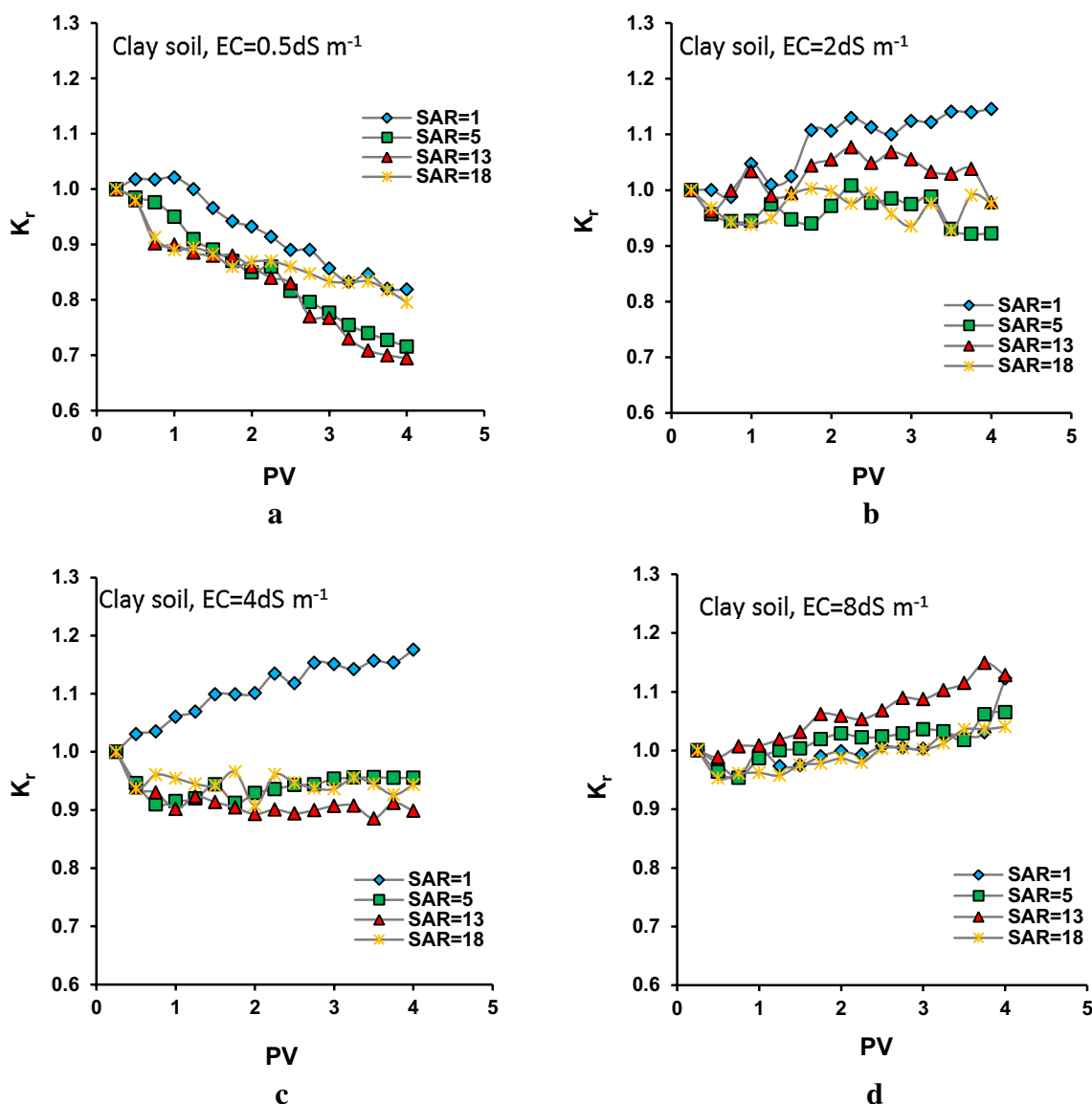
Fig. 1 Effect of SAR_w on relative hydraulic conductivity (K_r) versus pore volume (PV) for clay soil at different EC_w values: **a** 0.5, **b** 2, **c** 4 and **d** 8 dS m^{-1}
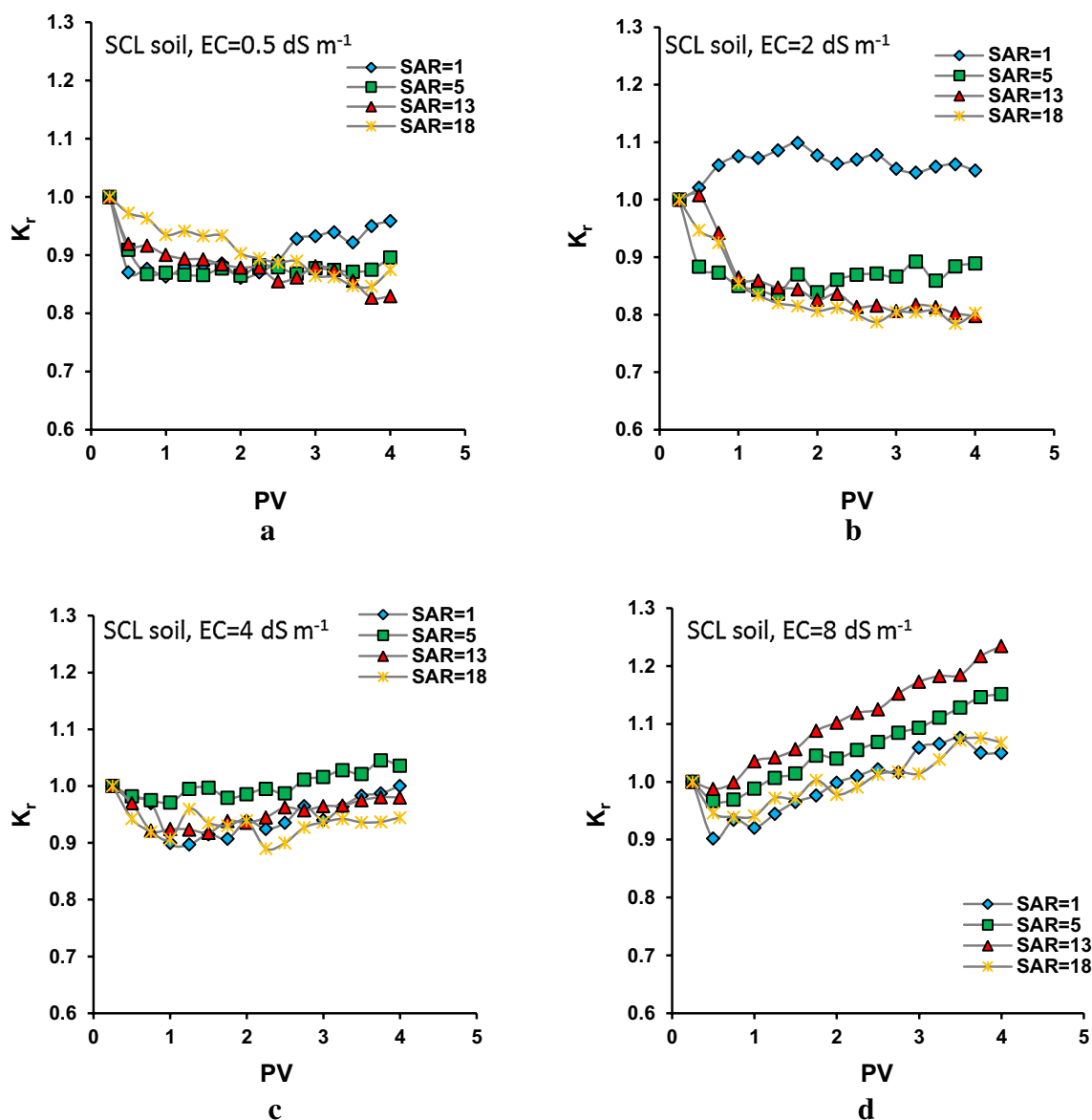
Fig. 2 Effect of SAR_w on relative hydraulic conductivity (K_r) versus pore volume (PV) for the sandy clay loam soil at different EC_w values: **a** 0.5, **b** 2, **c** 4 and **d** 8 dS m^{-1}

particles are flocculated ultimately affecting the pore sizes and continuity and hydraulic conductivity.

The effect of SAR_w at $EC_w = 4$ dS m^{-1} on K_r variation of the clay soil is shown in Fig. 1c. The K_r was minimally affected by the SAR_w, and the curves' slopes were near to zero due to counteracting impacts of salinity on sodicity. For low SAR_w (= 1), the K_r increased upon further leaching due to greater Ca^{2+} concentration compared to Na^+ concentration.

The effect of SAR_w at $EC_w = 8$ dS m^{-1} on K_r variation of the clay soil is shown in Fig. 1d. The high salinity and decreasing DDL thickness upon leaching increased the K_r. When compared with Fig. 1a–c, it is concluded that high

salinity minimized the impacts of sodicity on K_r so that even at high SAR_w, the K_r changes are negligible.

The effect of SAR_w at $EC_w = 0.5$ dS m^{-1} on K_r variation of the sandy clay loam soil is shown in Fig. 2a. It is seen that K_r decreased upon leaching with low-saline and high-sodic waters. The decreasing trend of K_r upon leaching was smaller when compared with Fig. 1a indicating the higher susceptibility of the clay soil to water quality. The clay soil has more clay particles and surface area, which make it susceptible to soil solution composition. Comparing Fig. 2a, b shows that for $SAR_w = 1$, the positive effect of EC_w on K_r was noticeable but not for the other SAR_w values having negative slope of K_r versus PV relation.

For EC_w of 4 dS m^{-1}, the K_r was almost constant upon leaching (Fig. 2c), indicating that when sodicity is high (i.e., $SAR_w = 18$) the EC_w should be at least 4 dS m^{-1} to preserve soil physical quality, and pore structure and continuity as quantified by hydraulic conductivity. When EC_w of 8 dS m^{-1} was used, the effect of leaching on K_r was positive irrespective of water sodicity.

Overall, with an increase in EC_w the K_r increased so that at high salinities (i.e., EC_w of 4 and 8 dS m^{-1}), EC_w could diminish the negative impact of SAR_w on soil structure and even increased the K_r to values greater than 1 upon leaching. Many investigators also reported that hydraulic conductivity increased with increasing electrolyte concentration and decreased with increasing SAR (Bagarello et al. 2006). In fact, swelling, aggregate failure, pore-size reduction and dispersion of clays are induced by the irrigation with low-quality water.

As leaching continued, the ion exchange between soil exchangeable sites and leaching solution increased and the differences between the treatments became greater. At high salinity (i.e., 8 dS m^{-1}), the effect of sodicity was not significant. Also at low salinity (i.e., 0.5 dS m^{-1}), there was no difference between SAR_w treatments because low concentrations of leaching solution itself lowered the K_r.

Other studies have also confirmed these results (e.g., Gamie and De Smedt 2018; Lado and Ben-Hur 2009). For instance, Bourazanis et al. (2016) investigated the effect of irrigation with treated municipal wastewater and freshwater on K_s and showed that by increasing EC and decreasing SAR of irrigation water, the soil particles were flocculated and consequently K_s increased. However, these studies have not been evaluated the capability of ANNs to predict soil hydraulic conductivity as affected by water quality.

Statistical analysis of the effect of soil texture and water quality on K_r

Analysis of variance of the effects of soil texture and water quality on K_r at different pore volumes (PV) during leaching trials is presented in Table 2. It was observed that the soil

texture only affected the K_r at PV = 1 significantly. However, the EC_w significantly affected the K_r when the leaching continued (at PVs of 2, 3 and 4). The SAR_w only affected the K_r at PV = 4 ($p < 0.05$). It seems that when the leaching continues, the incoming solution approached the equilibrium with the exchange sites of clay particles and consequently affected the soil structure and K_r. The interaction between soil texture and EC_w on K_r was significant ($p < 0.1$) at PV = 3. The interaction between soil texture and SAR_w on K_r was significant ($p < 0.1$ and 0.05) at PV of 0.5 and 1. The third-order interaction was only significant ($p < 0.1$) at PV = 1.

Table 3 shows the mean comparisons of the treatment effects on K_r at different PVs during leaching trials. The texture significantly affected the K_r only at 1PV. The mean K_r of sandy clay loam soil was greater than clay soil due to the effect of higher macropores and lower effect of water quality on microstructure of sandy clay loam soil. The effect of EC_w on K_r was not significant at 0.5PV and 1PV, but as the leaching proceeded, the EC_w increased the K_r. The K_r was greatest at EC_w of 8 dS m^{-1} which had significant

Table 3 Mean comparisons of the effects of soil texture and water quality on relative hydraulic conductivity (K_r) at different pore volumes (PV) during leaching trials

Texture	0.5PV	1PV	2PV	3PV	4PV
Clay	0.962[a]	0.981[a]	0.977[a]	0.984[a]	0.998[a]
Sandy clay loam	0.936[a]	0.926[b]	0.942[a]	0.963[a]	0.986[a]
EC_w (dS m^{-1})					
0.5	0.938[a]	0.942[a]	0.892[b]	0.864[b]	0.834[c]
2	0.979[a]	0.956[a]	0.967[a]	0.964[a]	0.980[b]
4	0.944[a]	0.995[a]	0.966[a]	1.020[a]	1.039[ab]
8	0.934[a]	0.968[a]	1.013[a]	1.040[a]	1.107[a]
SAR_w (meq l^{-1})$^{0.5}$					
1	0.965[a]	0.960[a]	0.987[a]	1.006[a]	1.048[a]
5	0.964[a]	0.969[a]	0.965[a]	1.001[ab]	1.038[ab]
13	0.944[a]	0.959[a]	0.959[a]	0.966[ab]	0.944[bc]
18	0.949[a]	0.925[a]	0.928[a]	0.919[b]	0.938[c]

In each group and column, means with at least one similar letter are not significantly different at $p < 0.05$ (Duncan multiple range test)

Table 2 Analysis of variance of the effects of soil texture and water quality on relative hydraulic conductivity (K_r) at different pore volumes (PV) during leaching trials

Source of variance	df	F ratio				
		0.5PV	1PV	2PV	3PV	4PV
Texture	1	1.79	7.84**	2.25	0.53	0.14
EC	3	1.13	0.32	4.60**	8.18**	11.18**
SAR	3	0.28	0.95	1.09	2.03*	3.13*
Texture×EC_w	3	0.19	0.35	2.08	2.22†	3.09
Texture×SAR_w	3	2.32†	3.75*	2.04	0.52	0.20
EC_w×SAR_w	9	0.88	0.85	1.17	1.39	1.68
Texture×EC_w×SAR_w	9	1.65	1.93†	1.35	1.16	0.42

†,* and ** stand for significant effects at 10, 5 and 1% probability levels, respectively

difference with other EC_w values. Comparing the effects of SAR_w values showed that at PV of 3 and 4, there were significant differences between K_r means with the highest K_r for $SAR_W = 1$. Upon leaching, the sodium had enough time to be adsorbed on the colloid surfaces and caused swelling and dispersion. These in addition to pore clogging (due to dispersed materials) decreased the K_r.

Table 4 shows the mean comparisons of the interactive effects of soil texture and EC_w on K_r at different PVs during leaching trials. The effect was not significant at 0.5PV and 1PV, but at other PVs, the K_r was significantly different among the texture–salinity combinations with the highest value observed for sandy clay loam soil leached with EC_w of 8 dS m^{-1}. The lowest K_r value belonged to clay soil leached with EC_w of 0.5 dS m^{-1}. The highest effect of EC_w was observed at 4PV due to greater leaching and the fact that the cations had enough time to be adsorbed on the colloid surfaces. As EC_w increases, the thickness of diffuse double layer (DDL) around the particles decreases leading to flocculation.

The interactive effects of soil texture and SAR_w on K_r at different PVs indicate that the K_r was lowest for both soils at $SAR_w = 18$ (Table 4). The effect was not significant at 4PV partly due to variability among the replicates and partly due to increase in hydraulic conductivity upon clay particles leave from the soil columns during leaching (which was visually observed).

Table 5 shows the mean comparisons of the interactive effects of EC_w and SAR_w on K_r at different PVs during leaching trials. Again the effect was not significant at 0.5PV and 1PV, but at other PVs, the K_r was significantly different among the salinity–sodicity combinations with the highest value observed for the high-salinity and low-sodicity treatments.

The K_s and K_r prediction using multiple regression and ANNs

Multiple regression analysis

The K_s and K_r were predicted from soil type, EC_w and SAR_w using multiple regression method, and the following two equations are derived:

$$K_s = 5.876047 - 0.00277\,EC_w - 0.04764\,SAR_w + 3.614373\,TEX - 0.00302\,PV$$

$$n = 512,\ R^2 = 0.629,\ MSE = 2.00,\ p < 0.000 \qquad (13)$$

$$K_r = 0.9366 + 0.014691\,EC_w - 0.00186\,SAR_w - 0.0326\,TEX - 0.00038\,PV$$

$$n = 512,\ R^2 = 0.240,\ MSE = 0.0068,\ p < 0.000 \qquad (14)$$

where K_s has the unit cm h^{-1}, the units of EC_w and SAR_w are dS m^{-1} and (meq l^{-1})$^{0.5}$, respectively, TEX stands for soil texture (0 for clay and 1 for sandy clay loam), and PV is number of pore volumes. It is obvious from Eqs. (13) and (14) that K_s prediction is more accurate than K_r prediction

Table 4 Mean comparisons of the interactive effects of soil texture and water quality on relative hydraulic conductivity (K_r) at different pore volumes (PV) during leaching trials

Texture		0.5PV	1PV	2PV	3PV	4PV
EC_w (dS m^{-1})						
Clay	0.5	0.952[a]	0.982[a]	0.896[b]	0.828[c]	0.782[c]
Clay	2	0.982[a]	0.989[a]	1.030[a]	1.025[a]	1.056[a]
Clay	4	0.968[a]	0.962[a]	0.956[ab]	1.046[a]	1.068[a]
Clay	8	0.946[a]	0.990[a]	1.033[a]	1.036[a]	1.089[a]
Sandy clay loam	0.5	0.924[a]	0.902[a]	0.888[b]	0.899[c]	0.904[bc]
Sandy clay loam	2	0.976[a]	0.923[a]	0.901[b]	0.903[bc]	0.905[bc]
Sandy clay loam	4	0.921[a]	0.934[a]	0.976[ab]	0.995[ab]	1.010[ab]
Sandy clay loam	8	0.923[a]	0.945[a]	1.004[a]	1.056[a]	1.125[a]
SAR (meq l^{-1})$^{0.5}$						
Clay	1	1.001[a]	1.042[a]	1.048[a]	1.045[a]	1.074[a]
Clay	5	0.965[ab]	0.977[ab]	0.946[ab]	0.998[ab]	1.044[a]
Clay	13	0.948[ab]	0.938[bc]	0.975[ab]	0.965[ab]	0.934[a]
Clay	18	0.932[ab]	0.964[abc]	0.942[b]	0.930[ab]	0.943[a]
Sandy clay loam	1	0.889[b]	0.878[c]	0.925[b]	0.967[ab]	1.023[a]
Sandy clay loam	5	0.963[ab]	0.973[ab]	0.984[ab]	1.005[ab]	1.033[a]
Sandy clay loam	13	0.941[ab]	0.944[bc]	0.946[ab]	0.967[ab]	0.952[a]
Sandy clay loam	18	0.953[ab]	0.913[bc]	0.914[b]	0.909[b]	0.933[a]

In each group and column, means with at least one similar letter are not significantly different at $p < 0.05$ (Duncan multiple range test)

using multiple regression technique. The effect of EC_w on K_s was negative and on K_r was positive. The impact of SAR_w on both K_s and K_r was negative. The coarser the texture, the higher the K_s was and the lower the K_r was. The effect of PV on both K_s and K_r was negative.

Artificial neural networks analysis

Two types of FFBP and CFBP neural networks have been implemented in this study. Two strategies were applied to find the best combination of different threshold functions in network optimization which included uniform threshold function for all layers (Table 6) and different threshold functions for layers (Table 7). Both two strategies

Table 5 Mean comparisons of the interactive effects of EC_w and SAR_w on relative hydraulic conductivity (K_r) at different pore volumes (PV) during leaching trials

EC_w (dS m^{-1})	SAR (meql^{-1})$^{0.5}$	0.5PV	1PV	2PV	3PV	4PV
0.5	1	0.955[a]	0.967[a]	0.916[b]	0.911[b]	0.912[bc]
0.5	5	0.952[a]	0.940[a]	0.861[b]	0.834[a]	0.814[c]
0.5	13	0.920[a]	0.941[a]	0.896[b]	0.854[b]	0.791[c]
0.5	18	0.924[a]	0.919[a]	0.895[b]	0.855[b]	0.853[c]
2	1	0.966[a]	0.945[a]	0.973[ab]	0.996[ab]	1.015[ab]
2	5	1.013[a]	1.022[a]	1.042[a]	1.039[a]	1.109[ab]
2	13	0.981[a]	0.956[a]	0.951[ab]	0.949[ab]	0.905[bc]
2	18	0.957[a]	0.895[a]	0.901[b]	0.872[b]	0.891[c]
4	1	0.985[a]	0.965[a]	1.048[a]	1.078[a]	1.124[ab]
4	5	0.964[a]	0.974[a]	0.981[ab]	1.132[a]	1.187[a]
4	13	0.890[a]	0.920[a]	0.911[b]	0.939[b]	0.897[c]
4	18	0.938[a]	0.934[a]	0.924[ab]	0.932[b]	0.948[bc]
8	1	0.894[a]	0.964[a]	1.079[a]	1.040[a]	1.143[a]
8	5	0.907[a]	0.934[a]	0.974[ab]	1.001[ab]	1.043[ab]
8	13	0.951[a]	1.020[a]	1.009[ab]	1.130[a]	1.182[a]
8	18	0.986[a]	0.957[a]	0.990[ab]	1.012[ab]	1.060[ab]

In each group, means with at least one similar letter are not significantly different at $p < 0.05$ (Duncan multiple range test)

Table 6 Learning algorithm for different neurons and hidden layers for the networks at the uniform threshold function

Network	Training algorithm	Threshold function	No. of layers and neurons	MSE	R^2	MAE	SD_{EMA}	Epoch
FFBP	LM	TANSIG	4–5–5–1	0.0011	0.9833	0.2860	0.2596	30
		LOGSIG	4–3–3–1	0.0692	0.9374	0.5662	0.6114	29
	BR	TANSIG	4–4–4–1	0.0005	0.9913	0.1641	0.2057	128
		LOGSIG	4–6–4–1	0.0006	0.9805	0.1854	0.1879	53
CFBP	LM	TANSIG	4–6–3–1	0.0004	0.9926	0.1512	0.1501	36
		LOGSIG	4–7–5–1	0.0511	0.9245	0.5743	0.5815	49
	BR	TANSIG	4–6–4–1	0.0005	0.9913	0.1641	0.2057	128
		LOGSIG	4–5–4–1	0.0461	0.9405	0.4140	0.4215	49

Table 7 Learning algorithm for different neurons and hidden layers for several networks at the different threshold functions

Network	Training algorithm	Threshold functions	No. of layers and neurons	MSE	R^2	MAE	SD_{EMA}	Epoch
FFBP	LM	TANSIG–LOGSIG–TANSIG	4–6–4–1	0.0010	0.9771	0.2476	0.2549	42
	BR	LOGSIG–LOGSIG–TANSIG	4–6–5–1	0.0007	0.9807	0.2257	0.2210	49
CFBP	LM	LOGSIG–LOGSIG–TANSIG	4–5–4–1	0.0003	0.9945	0.1761	0.1715	29
	BR	LOGSIG–TANSIG–TANSIG	4–4–4–1	0.0008	0.9792	0.2253	0.2459	32

were used in training of FFBP and CFBP networks with learning algorithms of LM and BR. The best results of employed networks and algorithms for first and second strategies are presented in Tables 6 and 7, respectively. It is observed that the performance of ANNs is much greater than regression method for K_s prediction.

The best results of FFBP network with LM algorithm in the first strategy with TANSIG threshold function was related to 4–5–5–1 topology (Table 6). This composition produced MSE $= 0.0011$, $R^2 = 0.9833$ and MAE $= 0.2860$ and converged in 30 epochs. In addition, the best result of this network with BR algorithm in first strategy was obtained with TANSIG threshold function and 4–4–4–1 topology. This composition has MSE $= 0.0005$, $R^2 = 0.9913$ and MAE $= 0.1641$. This composition converged in 128 epochs. Furthermore, in this stage, BR learning algorithm had better result, because it produced lower MAE and higher R^2 values. It was found that, in both strategies for FFBP network, TANSIG threshold function presented the better performance (in terms of error and R^2 values) for similar initial conditions.

The results for CFBP network in first strategy showed that the LM algorithm had better performance compared to BR algorithm. The best result for LM algorithm was derived for 4–6–3–1 topology with MAE $= 0.0004$ and $R^2 = 0.9926$ at 36 training epochs, whereas the best results belonged to 4–6–4–1 topology for BR algorithm. It produced MAE $= 0.1641$, $R^2 = 0.9913$ at 128 epochs. With regard to first strategy results, the best topology (4–6–3–1) is belonged to CFBP network with LM algorithm and TANSIG threshold.

The best result for second strategy and FFBP network and LM algorithm is related to 4–6–4–1 topology and TANSIG–LOGSIG–TANSIG threshold functions (Table 7). This composition has MAE $= 0.2476$, $R^2 = 0.9771$. For BR algorithm, the best topology is 4–6–5–1 with LOGSIG–LOGSIG–TANSIG threshold functions. It produces MAE $= 0.2257$, $R^2 = 0.9807$ at 49 epochs. Furthermore, for FFBP network, BR algorithm has better result compared to LM algorithm. The CFBP network for second strategy, LM algorithm, 4–5–4–1 topology and threshold functions of LOGSIG–LOGSIG–TANSIG has MAE $= 0.1761$ and $R^2 = 0.9945$. In addition, the BR algorithm with FFBP network and 4–4–4–1 topology with LOGSIG–TANSIG–TANSIG threshold functions produced MAE $= 0.2253$ and $R^2 = 0.9297$. According to the results of second strategy, CFBP network with LM algorithm, as an optimized topology, had the best performance, which was superior to the first strategy, because the MAE and R^2 are higher. The R^2 of optimized ANN is plotted in Fig. 3.
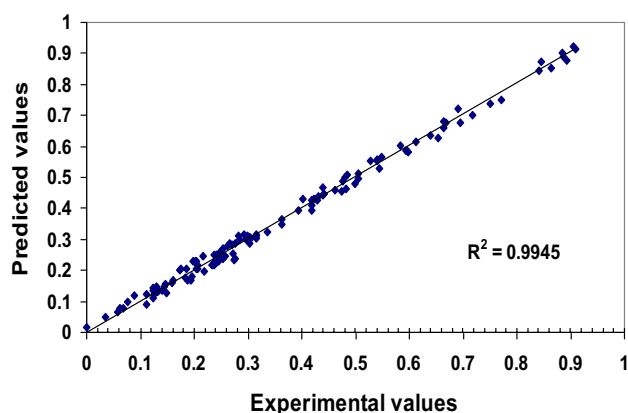

Fig. 3 Predicted values of K_s using ANNs versus measured values for testing data

Conclusions

1. The K_s values were greater in sandy clay loam soil due to more macropores compared to clay soil. With an increase in SAR$_w$, the K_s decreased due to soil dispersion, macropore clogging by dispersed clay particles and swelling.

2. As leaching was continued (at high PVs), the K_r decreased because the low-saline waters could disperse soil aggregates. The effect was greater when the waters with high SAR$_w$ values were used. When the SAR$_w$ reached to 13, the K_r decrease was substantial, especially at initial PVs. There was an increase in the K_r for SAR $= 18$, especially at high PVs presumably because of particles separation and creation of new pores upon extensive swelling.

3. For the clay soil, it was observed, by comparing K_r reductions at EC$_w = 2$ dS m^{-1} and EC$_w = 0.5$ dS m^{-1}, that increase in salinity compensated the reduction of K_r due to SAR$_w$. The effect of leaching with moderately saline water on K_r was positive, especially at low SAR$_w$ values. However, K_r was minimally affected by the SAR$_w$ at EC$_w = 4$ dS m^{-1}. Results showed that if leaching continues by water with low SAR$_w$ ($= 1$), K_r will be increased. In generally, even in the conditions of clay soil and high SAR$_w$, impact of sodicity on K_r was minimized by high salinity. The clay soil was more sensitive to water quality when compared with the sandy clay loam soil. It was founded that in the case of high sodicity (SAR$_w = 18$), the EC$_w$ must be at least 4 dS m^{-1} to preserve the soil physical quality, pore structure and continuity as quantified by the saturated hydraulic conductivity.

4. For the highest EC$_w$, K_r values of both soil textures were increased during leaching even at the highest SAR$_w$ value. Therefore, it can be concluded that EC$_w$ has more effect on soil structure than SAR$_w$ does.

5. The effects of soil type and water quality on the K_s were effectively predicted by regression and ANN methods. It was observed that the efficacy of ANNs is much greater than regression method for K_s prediction. Results of ANNs with regard to second strategy showed that the best topology (4–5–4–1) is belonged to CFBP network with LM algorithm and LOGSIG–LOGSIG–TANSIG threshold functions. In this method, the MAE and R^2 were 0.1761 and 0.9945, respectively.

References

Agyare WA, Park SJ, Vlek PLG (2006) Artificial neural network estimation of saturated hydraulic conductivity. Soil Sci Soc Am J 6:423–431

Bagarello V, Iovino M, Palazzolo E, Panno M, Reynolds WD (2006) Field and laboratory approaches for determining sodicity effects on saturated soil hydraulic conductivity. Geoderma 130:1–13

Bourazanis G, Katsileros A, Kosmas C, Kerkides P (2016) The effect of treated municipal wastewater and fresh water on saturated hydraulic conductivity of a clay-loamy soil. Water Resour Manag 30:2867–2880

Buelow MC, Steenwerth K, Parikh SJ (2015) The effect of mineral-ion interactions on soil hydraulic conductivity. Agric Water Manag 152:277–285

Chayjan RA, Esna-Ashari M (2010) Comparison between artificial neural networks and mathematical models for equilibrium moisture characteristics estimation in raisin. Agric Eng Int CIGR E J 12:1305–1319

Demuth H, Beale M, Hagan M (2007) Neural network toolbox 5 user's guide. The Mathworks Inc, Natrick

Emdad MR, Rain RS, Smith RJ, Fardad H (2004) Effect of water quality on soil structure and infiltration under furrow irrigation. Irrig Sci 23:55–60

Erzin Y, Gumaste SD, Gupta A, Singh DN (2009) Artificial neural network (ANN) models for determining hydraulic conductivity of compacted fine-grained soils. Can Geotech J 46:955–968

Gamie R, De Smedt F (2018) Experimental and statistical study of saturated hydraulic conductivity and relations with other soil properties of a desert soil. Eur J Soil Sci 69:256–264

Girosi F, Jones M, Poggio T (1995) Regularization theory and neural network architectures. Neural Comput 7:219–269

Green TR, Ahuja LR, Benjamin JG (2003) Advances and challenges in predicting agricultural management effects on soil hydraulic properties. Geoderma 116:3–27

Heristev RM (1998) The ANN book. GNU Public License. ftp://funet.fi/pub/sci/neural/books/. Accessed Apr 3, 2005

Kaveh M, Chayjan RA, Nikbakht AM (2017) Mass transfer characteristics of eggplant slices during length of continuous band dryer. Heat Mass Transf 53:2045–2059

Keren R, Ben-Hur M (2003) Interaction effects of clay swelling and dispersion and $CaCO_3$ content on saturated hydraulic conductivity. Aust J Soil Res 41:979–989

Klute A (1986) Methods of soil analysis, part 1, physical and mineralogical properties, ASA/Soil Sci Society Am, Monograph 9, 2nd edn, Madison

Lado M, Ben-Hur M (2009) Treated domestic sewage irrigation effects on soil hydraulic properties in arid and semiarid zones: a review. Soil Tillage Res 106:152–163

Levy GJ, Rosenthal A, Tarchitzky J, Shainberg I, Chen Y (1999) Soil hydraulic conductivity changes caused by irrigation with reclaimed waste water. J Environ Qual 28:1658–1664

Levy GJ, Goldstein D, Mamedov AI (2005) Saturated hydraulic conductivity of semiarid soils. Soil Sci Soc Am J 69:653–662

Lim DKHP, Kolay K (2009) Predicting hydraulic conductivity (k) of tropical soils by using artificial neural network (ANN). UNIMAS E-J Civ Eng 1:1–6

Love M (2017) Use of NARX neural networks to forecast daily groundwater levels. Water Resour Manag 31(5):1591–1603

Mossadeghi-Björklund M, Arvidsson J, Keller T, Koestel J, Lamandé M, Larsbo M, Jarvis N (2016) Effects of subsoil compaction on hydraulic properties and preferential flow in a Swedish clay soil. Soil Tillage Res 156:91–98

Page AL, Miller RH, Keeney DR (1992) Methods of soil analysis. Part 2. Chemical and microbiological properties, Agron. Monog. 9. 2nd edn. ASA/Soil Sci Soc Am J, Madison

Parasuraman K, Elshorbagy A, Si BC (2006) Estimating saturated hydraulic conductivity in spatially variable fields using neural network ensembles. Soil Sci Soc Am J 70:1851–1859

Raheli B, Aalami MT, El-Shafie A, Ghorbani MA, Deo RC (2017) Uncertainty assessment of the multilayer perceptron (MLP) neural network model with implementation of the novel hybrid MLP-FFA method for prediction of biochemical oxygen demand and dissolved oxygen: a case study of Langat river. Environ Earth Sci 76:503

Sivanandam SN, Sumathi S, Deepa SN (2006) Introduction to neural networks using Matlab 6.0. Tata McGraw-Hill Publishing Company Limited, Hyderabad

Suarez DL, Wood JD, Lesch SM (2006) Effect of SAR on water infiltration under a sequential rain-irrigation management system. Agric Water Manag 86:150–164